Journal of the Nigerian Association of Mathematical Physics
Volume 57(**June – July** *2020 Issue*), **pp67 – 76**

APPROXIMATE SOLUTION OF A MAGNETOHYDRODYNAMIC NATURAL CONVECTION OF FLUID WITH VARIABLE PROPERTIES, MAGNETIC INDUCTION, VISCOUS AND OHMIC DISSIPATION AND SUCTION.

A. O. Ajibade[1] and A. B. Shehu[2]

[1]Department of Mathematics, Ahmadu Bello University, Zaria, 810107 Nigeria.
[2]Depart.ment of Mathematics and Statistics, Kaduna Polytechnics, Kaduna, 1000014 Nigeria

Abstract

In this paper the effect of suction, viscous dissipation and Ohmic heating on magnetohydrodynamic (MHD) free convection flow of an electrically conduction fluid with the combined effect of variable thermal conductivity and viscosity in a vertical porous channel with induced magnetic field are studied by the use of the differential transform method. The fluid is conditioned to a uniform suction and transverse magnetic field through the plates. Viscous dissipation is considered present due to the heat generated from the interaction of fluid molecules next to each other due to shear forces. Ohmic heating is also considered to take place as a result of the electrical resistance of the flowing fluid due to the presence of electric current. The effects of suction, variable viscosity, variable thermal conductivity and the other parameters involved in the study are tested on the velocity, temperature and the induced magnetic field profiles. This is made possible after solving the governing transformed ordinary differential equations. It is found that when suction of the fluid decreases, its velocity profile decreases as it does when the viscosity of the fluid is increased. Also, an increase in the suction of the fluid increases the induced magnetic field.

***Keywords*: -** *Viscous and Ohmic dissipation, suction, induced magnetic field and differential transform method (DTM).*
PACS: - 47.65.-d, 44.25.+f, 44.30.+v, 47.56.+r,

Table 1 Nomenclature

U velocity of the fluid	μ^* Variable viscosity of the fluid
h channel width(gab between the plates)	β Coefficient if thermal expansion
$B'_{x'}$ Induced Magnetic field in the x' direction	ρ Density of the fluid
B_0 constant magnetic flux density	v Fluid kinematic viscosity
g gravitational acceleration	σ Electrical conductivity of the fluid
Ha Hartmann number	μ_e Magnetic permeability
J Induced current density	κ^* Variable thermal conductivity of the fluid
Nu Nusselt number	λ viscosity-variation parameter
T Temperature of the fluid	ε Thermal conductivity variation parameter
u' Velocity of the fluid along x' axis	τ Skin friction coefficient
v' Velocity of fluid along the y' axis	
T_0 Reference temperature	
Pm magnetic Prandtl number	
Pr Prandtl number	
V Suction velocity	

1. INTRODUCTION

Flows through porous media, have wide applications and they play very important roles in many Engineering and geophysical applications. These include the field of chemical engineering for filtration and purification processes; in the field of agricultural engineering to investigate the underground water resources; in petroleum industry to study the movement of natural gas, oil and water through channels and reservoirs. A significant number of researches have been carried out on natural convection MHD flows in porous

Corresponding Author**:** Shehu A.B., Email: bolajishehu13@gmail.com, Tel: +2348037055220

channels. Such as, the effects of hall current and viscous dissipation on magneto hydrodynamic natural convection fluid flow in a rotary system. This was discussed in [1], where the explicit finite difference solution method was used to deduce that, the primary velocity of the flow increases with the increase of the Eckert number while it decreases with the increase of the magnetic parameter and the Prandtl number. Analysis of Ohmic and viscous heating on non-Darcy MHD free convection flow from a cylinder with porosity and internal heat generation was studied in [2] using the Keller-box finite difference scheme. It is discovered that when the viscous dissipation parameter (Ec) is increased, the velocity is increased. Semi-implicit finite difference method was used in the work conducted in [3] to solve the governing equation obtained from the study of the effects of suction and injection, on unsteady MHD convective viscous flow between porous media with thermal diffusion. This leads to the conclusion that the velocity of the flow is slowest near the wall where suction takes place and fastest close to the wall where injection takes place. Also, in [4] Runge-Kutta together with the shooting method was used to investigate viscous dissipation and mass transfer effects on unsteady MHD natural convection flow along a moving vertical porous plate in the presence of internal heat generation and variable suction. It is discovered that the temperature of the fluid decreases when the Prandtl number or suction parameter increases. The investigation in [5] of MHD free convection flow, over a semi-infinite porous medium, with heat absorption and chemical reaction, led to the conclusion that the velocity of the fluid increases when the permeability parameter of the porous medium is enhanced. The conclusion that **t**he temperature distribution of a flowing fluid decreases as Prandtl number is increased was reached in [6] when MHD natural convection flow over an infinite porous media with a transverse magnetic field and constant heat flow density was discussed. It is also argued that the temperature as well as velocity increased due to increase in viscous dissipative parameter when in [7] MHD free convection and mass transfer flow, over an infinite vertical porous plate, with viscous dissipation was studied. The investigation on Magneto-hydrodynamic flow with viscous dissipation and chemical reaction over a stretching porous plate in porous medium was conducted in [8], using the BVP4C numerical method to solve the governing equation, and deduced that the magnetic parameter decreases the velocity, whereas it has increasing effect on temperature. In [9], Series expansion method was employed in discussing the effect of suction and injection on MHD three dimensional couette flows and heat transfer through a porous medium. Arguing that an increasing magnetic parameter slows down the main velocity and accelerates the cross flow velocity of the flow field. While a growing permeability, parameter or suction and injection parameter reverses the effect. Hall current effects on free convective flow of stratified fluid over an infinite vertical porous plate was discussed in [10] and explained that the skin friction in general, decreases with increase in all the parameters of interest. Conclusions are also reached in [11], that because of the inclusion of variable properties on magneto hydrodynamic heat transfer close to a stagnation point, along a stretching sheet in a porous medium with heat radiation, a considerable rise in the velocity profile and a significant reduction in the temperature and concentration profiles inside the boundary layer occur. In addition, it is observed that the presence of fluid suction increases the rate of heat transfer. Fluid velocity increases with heat generation or with increase in the electrical conductivity parameter, while it decreases due to increase in magnetic field intensity. This is the conclusion from the work in [12] on steady magneto hydrodynamics free convective flow of an electrically conducting fluid heat generation along an isothermal plate. The effects of viscous and joule heating on magneto-hydrodynamic flow through a stretching porous surface embedded in a porous medium was conducted in [13] and the results show that increase in magnetic parameter decrease both the dimensionless velocity and the skin friction coefficient.

In most of the studies above, either the viscosity and thermal conductivity are considered constants or one of them is considered to vary with temperature while the other does not. However, it is a known fact that these physical properties are temperature dependent. To determine precisely, the behavior of the flowing fluid, the realistic dependence of the viscosity and the thermal conductivity of the fluid on temperature are necessary to take into account. Hence, it is observed that increase in the viscosity of fluids increases the rate of the heat transfer as showcased in [14] concerning temperature dependent viscosity on Magneto-hydrodynamic natural convection flow at an axis-symmetric stagnation point saturated in porous media. Just like viscosity, it is evident that thermal conductivity is a function of temperature [15]. In the study undertaken in [16] on the effects of temperature dependent heat conductivity and viscosity on magneto-hydrodynamics mixed convective flow over a surface with radiation, it is discovered that velocity and temperature vary significantly with the variation of viscosity and heat conductivity parameters. The theoretical study conducted herein, discusses combined effect of variable thermal conductivity and temperature dependent viscosity on MHD natural convection flow in vertical porous channel with induced magnetic field, Ohmic and viscous dissipation. The transformed governing boundary value equations involving the velocity, temperature and the induced magnetic fields are solved numerically by the differential transform method. In addition, the expression for the induced current density, the skin friction and the Nusselt number are obtained. The pertinent results are displayed in graphs, tables and discussed quantitatively.

2. THEORETICAL ANALYSIS

Consider a steady natural convection boundary layer flow of a viscous, electrically conducting and incompressible fluid with variable viscosity; variable thermal conductivity with induced magnetic field, Ohmic and viscous dissipation through two infinitely long vertical porous plates with constant suction whose suction velocity is given by V_0' as depicted in figure 1 below.

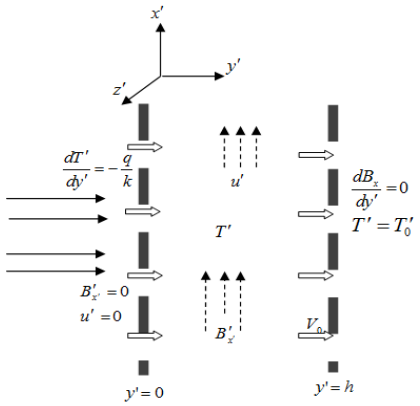

Figure 1. Geometry of the problem.

Taking u' and v' as the components of the velocities x' (along the plates) and y' (normal to the plates), respectively and h the distance between the two permeable vertical plates as shown in figure 1. Then, keeping one of the plates at constant heat flux $\left(\frac{-q}{k}\right)$ and the other maintained at constant temperature T_0' , so that for the steady incompressible boundary layer flow, the governing equations can be written as done in [17] shown below.

$$\frac{1}{\rho}\frac{d}{dy'}\left(\mu^*\frac{du'}{dy'}\right)+\frac{\mu_e B_0}{\rho}\frac{dB'_{x'}}{dy'}+g\beta\left(T'-T_0'\right)+V_0'\frac{du'}{dy'}=0 \tag{6}$$

$$\frac{1}{\sigma\mu_e}\frac{d^2B'_{x'}}{dy'^2}+B_0'\frac{du'}{dy'}+V_0'\frac{dB'_{x'}}{dy'}=0 \tag{7}$$

$$\frac{1}{\rho C_p}\frac{d}{dy'}\left(k^*\frac{dT'}{dy'}\right)+\frac{\mu^*}{\rho C_p}\left(\frac{du'}{dy'}\right)^2+\frac{J^2}{\rho C_p\sigma}+V_0'\frac{dT'}{dy'}=0 \tag{8}$$

With the boundary conditions

$$u'=0, B'_{x'}=0, \frac{dT'}{dy'}=-\frac{q}{k^*}, at, y'=0 \tag{9}$$

$$u'=0, \frac{dB'_{x'}}{dy'}=0, T'=T_0', at, y'=h \tag{10}$$

μ^* and k* represents the velocity and thermal conductivity of the fluid respectively. These are temperature dependent viscosity. Hence, making the present work different from that of [17] in which viscosity and thermal conductivity of the fluid are taken to be constants. V_0' is a constant with $V_0'>0$ representing the suction velocity at the plate surface. $V_0'<0$ corresponds to injection. The fluid density is represented by ρ; C*p* is the specific heat of the fluid at constant pressure. Because of the fluid's electrical conductivity (σ) a magnetic field $B'_{x'}$ is induced along the $x'-axis$. Equation (6) above is the expression for the velocity field with the temperature dependent viscosity taken as an inverse linear function of temperature following the study in [16] as

$$\frac{1}{\mu^*}=\frac{1}{\mu_0}\left(1+a\left(T'-T_0\right)\right) \tag{11}$$

Where, a *and* T_0 are constants. Equation (11) is equivalent to equation (12) below

$$\mu^*=\mu_0\left(1-a\left(T'\Delta T\right)\right). \tag{12}$$

Equation (7) is the expression for the induced magnetic field and equation (8) is the expression for the temperature field with the variable thermal conductivity taken as an inverse linear function of temperature following the work in [18] as

$$\frac{1}{k^*}=\frac{1}{k_0}\left(1+b\left(T'-T_0\right)\right). \tag{13}$$

This can be written as equation (14) below

$$k^*=k_0\left(1-b\left(T'\Delta T\right)\right). \tag{14}$$

a,b and T_0 are constants and their values depend on the reference state and the properties displayed by the fluid when heat is passed through it. Also, for liquids $a>0$ and for gases $a<0$; μ_0 is the dynamic viscosity and k_0 thermal conductivity of the fluid far away from the wall (ambient fluid).

From equation (12) let λ = aΔT which is the viscosity variation parameter. It is obvious that it increases with increasing temperature. So that equation (10) becomes equation (13) below

$$\frac{\mu^*}{\mu_0}=\left(1-\lambda T'\right) \tag{15}$$

Equation (15) shows that the value of the dimensionless viscosity $\left(\frac{\mu^*}{\mu_0}\right)$ decreases with increasing temperature. That is when $\lambda>0$.

Since the viscosity of liquids reduces with enhanced temperature while it increases for gases, λ is taking to be negative for liquids and positive for gases. Likewise, the same argument can be put forward for the dimensionless thermal conductivity. So that

$$\frac{k^*}{k_0}=\left(1-\varepsilon T'\right) \tag{16}$$

Where ε = bΔT is taking as the thermal conductivity variation parameter; and it is taken to be negative in liquids and positive in gases.

Using the non-dimensional parameters below

$$y=\frac{y'}{h}, u=\frac{\nu u'}{g\beta h^2\Delta T'}, B=\frac{\nu'}{g\beta h^2\Delta T'}\sqrt{\frac{\mu_e}{\rho}}B'_{x'}, T=\frac{T'-T_0'}{\Delta T'}, \Delta T'=\frac{hq}{k}, \tag{17}$$

$$\Pr=\frac{\mu C_p}{k}, Pm=\nu\sigma\mu_e, Ha=\frac{B_0h}{\nu}\sqrt{\frac{\mu_e}{\rho}}, V_0=\frac{V_0'h}{\nu}, \lambda=a\Delta T \ and \ \varepsilon=b\Delta T,$$

the equations governing the problem are transformed into the system of nonlinear ordinary differential equations of the second order below

$$\frac{d^2u}{dy^2} + Ha\,\frac{dB}{dy} - \lambda(1+\lambda T)\frac{dT}{dy}\frac{du}{dy} + (1+\lambda T)T + V\frac{du}{dy} = 0 \tag{18}$$

$$\frac{d^2B}{dy^2} + PmHa\,\frac{du}{dy} + VPm\,\frac{dB}{dy} = 0 \tag{19}$$

$$\frac{d^2T}{dy^2} - \varepsilon(1+\varepsilon T)\left(\frac{dT}{dy}\right)^2 + \Pr Ec(1-\lambda T)^2\left(\frac{du}{dy}\right)^2 + M^2\Pr Ec(1-\lambda T)u^2 + V\Pr\frac{dT}{dy} = 0 \tag{20}$$

And the boundary conditions are transformed to

$$u = 0, B = 0, \frac{dT}{dy} = -1, at, y = 0 \tag{21}$$

$$u = 0, \frac{dB}{dy} = 0, T = 0, at, y = 1 \tag{22}$$

EXPERIMENTAL WORK

In order to solve the non-linear governing continuity, momentum and energy equations, the equations (6) to (10) are reduced into ordinary differential equations (18) to (22) using the set of non-dimensional parameters (17). Hence, the non-linear second order coupled ordinary differential equations (18) to (22) are represented by the iterative relations (23) to (26) respectively using the Differential Transform Method. This is then coded into the symbolic software called Maple [19].

$$U(K+2) = \frac{K}{(K+2)!}\cdot\begin{pmatrix} \lambda\cdot\sum_{r=0}^{K}(r+1)\cdot(K-r+1)\cdot U(r+1)\cdot T(K-r+1) \\ +\lambda^2\cdot\sum_{r=0}^{K}\sum_{t=0}^{r}(t+1)\cdot(r-t+1)\cdot U(t+1)\cdot T(r-t+1)\cdot T(K-r) \\ -Ha\cdot(K+1)\cdot B(K+1) - T(K) \\ -\lambda\cdot\sum_{r=0}^{K}T(r)\cdot T(K-r) - V\cdot(K+1)\cdot U(K+1) \end{pmatrix} \tag{23}$$

$$B(K+2) = \frac{K}{(K+2)!}\cdot(-Pm\cdot(V\cdot(K+1)\cdot B(K+1) + Ha\cdot(K+1)\cdot U(K+1))) \tag{24}$$

$$T(K+2) = \frac{K!}{(K+2)!}\cdot\begin{pmatrix} \varepsilon\cdot\sum_{r=0}^{K}(r+1))\cdot(K-r+1)T(r+1)T(K-r+1) \\ +\varepsilon^2\cdot\sum_{r=0}^{K}\sum_{t=0}^{r}(t+1)\cdot(r-t+1)T(t+1)T(r-t+1)T(K-r) \\ -\Pr Ec\cdot\sum_{r=0}^{K}(r+1)(K-r+1)U(r+1)U(K-r+1) \\ +2\lambda\cdot\Pr Ec\sum_{r=0}^{K}\sum_{t=0}^{r}(t+1)(r-t+1)U(t+1)U(r-t+1)T(K-r) \\ -\lambda^2\cdot\Pr Ec\cdot\sum_{r=0}^{K}\sum_{t=0}^{r}\sum_{i=0}^{t}(i+1)(t-i+1)\cdot U(i+1)\cdot U(t-i+1)T(K-t)T(K-r) \\ -M^2\cdot\Pr Ec\cdot\sum_{r=0}^{K}U(r)U(K-r) \\ +M^2\cdot\Pr Ec\sum_{r=0}^{K}\sum_{t=0}^{r}(t+1)(r-t+1)U(t+1)U(r-t+1)T(K-t)T(K-r) \\ -V\cdot\Pr\cdot(K+1)T(K+1) \end{pmatrix} \tag{25}$$

Also, the boundary conditions give

U (0) = 0; U (1) = a; T (1) = -1; T (0) = c; B (0) = 0; B (1) = d. (26)

The symbols U (K), B (K) and T (K) are the differential transforms of U(y), B(y) and T(y) respectively. The unknowns a, c and are constants to be determined. Hence, the following respective polynomial results (27) to (30) are obtained.

$U(y) = a.y + (-(\frac{1}{2}).\lambda^2.a.c - -(1/2).\ \lambda.a.c^2 - (1/2).Ha.d\ - (1/2).V.a\ - (1/2).\ \lambda.a - (1/2).c).y^2 + \ldots$

$(1/2).Pm.H\ \ a.a - (1/2).V.Pm\ \ .d) + 1/6 + (1/3).\ \lambda.c - (1/3).V.(\ - (1/2).\ \lambda^2.a.c - (1/2).\ \lambda.c^2 - \ldots$ (27)

$(1/2).Ha.d\ - (1/2).V.a\ - (1/2).\ \lambda.a - (1/2).c).\ \ y^3 + \ldots$

$B(y) = d + (2.(\ - (1/2).Pm.H\ \ a.a - (1/2).V.Pm\ \ .d)).y\ + (3.(\ - (1/3).Pm.H\ \ a.(\ - (1/2).\ \lambda^2.a.c -$

$(1/2).\ \lambda^2.c^2 - (1/2).Ha.d\ - (1/2).V.a\ - (1/2).\ \lambda.a - (1/2).c)\ - (1/3).V.Pm\ \ .(\ - (1/2).Pm.H\ \ a.a$ (28)

$- (1/2).V.Pm\ \ .d))).y^2 + ...(1/3)\ .V.Pm.(\ - (1/2).Pm.H\ \ a.a - (1/2).V.Pm\ \ .d)))).y^3 + \ldots$

$T(y) = c - y + ((1/2).V.P\ \ r.\varepsilon.c + (1/2).\ \varepsilon^2.c + (1/2).V.Pr\ \ + (1/2).\ \varepsilon).y^2 + \ldots +$ (29)

$(1/6).V.Pr\ \ .\varepsilon.(1 + (2.((1/2).\ \ V.Pr.\ \varepsilon.c + (1/2).\ \ \varepsilon^2.c + (1/2).V.Pr\ \ + (1/2).\ \varepsilon)).c)).y^3 + \ldots$

From the polynomial equations (27) to (29), the induced current density, the local skin-friction coefficient and the local Nusselt number that are respectively given by J, τ and Nu, as presented in polynomial equations (30) to (36) are obtained and their numerical values are presented in tabular forms.

$$J = -dB/dy = -d - 2.(-(1/2).\ Pm.a.Ha - (1/2).V.Pm .d)).y - (3.(-(1/3) .Pm.Ha.(-(1/2).\ \lambda^2.a.c - (1/2).\ \lambda.c^2 - (1/2).Ha.d - (1/2).V.a - (1/2).\ \lambda.a - (1/2).c) - (1/3).V.Pm .(-(1/2).P m.a.Ha - (1/2).V.Pm .d))).y^2 + \ldots \quad (30)$$

$$\tau = (1-\lambda T)\left(\frac{dU}{dy}\right) \quad (31)$$

$$\tau = (- (c - y + ((1/2).V.P r.\varepsilon.c + (1/2).\ \varepsilon^2.c + (1/2).V.Pr + (1/2).\ \varepsilon).y^2 + \ldots \quad (32)$$

$$\tau_0 = (1-\lambda T).\left(\frac{dU}{dy}\right)_{y=0} = (-c.\lambda + 1).a \quad (33)$$

$$\tau_1 = -(1-\lambda T).\left(\frac{dU}{dy}\right)_{y=1} = (- (c - 1 + (1/2).V.Pr .\varepsilon.c + (1/2).\ \varepsilon^2.c + (1/2).V.Pr + (1/2).\ \varepsilon + \ldots + -(1/2).Pm.(Ha)^2.a - (1/2).V.Pm .Ha.d + \lambda.c + \ldots \quad (34)$$

The Nuselt number Nu is given by the equations (35) and (36).

$$Nu = (1-\varepsilon T).\left(\frac{dT}{dy}\right) = -c + y - (1/2.\ V.\ Pr.\varepsilon.c - 1/2.\ \varepsilon^2.c - 1/2\ .V.\ Pr - 1/2.\ \varepsilon).\ y^2 + \ldots \quad (35)$$

$$Nu = (1-\varepsilon T).\left(\frac{dT}{dy}\right)_{y=1} = (-(c - 1 + (1/2).V.Pr .\varepsilon.c + (1/2).\ \varepsilon.c + (1/2).V.Pr + (1/2).\ \varepsilon + (1/6).\ \varepsilon.(-2.Pr.V.c .\varepsilon - 2.c.\ \varepsilon^2 - 2.Pr.V - 2.\varepsilon) + \ldots \quad (36)$$

4. RESULTS AND DISCUSSIONS

The governing equations of a conducting magneto-hydrodynamic free convection flowing fluid, with dependent thermal conductivity and viscosity are solved. It is assumed that Magnetic induction, Joule and viscous heating, are present in the flow through a vertical porous channel. The solution is obtained by the Differential Transform Method (DTM) proposed in [20]. The DTM has also been successfully applied to solve various types of differential equations by many researchers as in the cases discussed in [20 - 24]. Using this method, the expressions for the velocity profile, magnetic field profile, temperature profile, induced magnetic field equation, the skin friction and the Nusselt number are determined. It is found in this work that the convergence of the iteration process is rapid. The convergence of the method being already established in [25]. Therefore, the velocity profiles (U), shown in figures (2) to (9); the induced magnetic field profiles (B), in figures (10) to (15); the temperature profiles (T), shown in figures (16) to (19) and the induced current density profile (J), depicted in figures (20) to (26), helps in the discussion of how the flow parameters causes changes on the velocity field, induced magnetic field, the temperature field and the induced current density respectively. Also, the effects of the relevant parameters on the skin friction (τ) and on the heat flux (Nu) are shown in tables (1) and (2) respectively. To validate the accuracy of our numerical procedure, we have compared our numerical results with the analytical solution results obtained in [17] by taking viscosity and thermal conductivity to be constants and neglecting the effects of viscous dissipation and Ohmic heating. It is shown in table 3 that the results are found to agree with each other. The flow parameters include the suction and injection parameter (V), variable viscosity parameter (λ), the variable thermal conductivity parameter(ε), the Eckert number (Ec), the magnetic parameter (M), the Prandtl number (Pr), the Hartmann number (Ha) and magnetic Prandtl number (Pm). For these parameters, the following ranges of values have been used for computations: $V\,(0.1 \le V \le 0.4)$, $\lambda\,(-1.0 \le \lambda \le -0.05)$, $\varepsilon\,(0.1 \le \varepsilon \le 0.4)$, $Pm\,(0.1 \le Pm \le 0.5)$, $Ha\,(1.0 \le Ha \le 4.0)$, $\Pr\,(0.7 \le \Pr \le 6.0)$, $Ec\,(0.1 \le Ec \le 1.5)$, $M\,(1.0 \le M \le 10.0)$

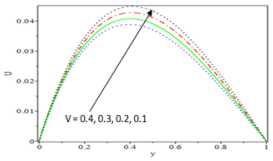

Figure 2 Velocity profile varying V for Ec = 0.1, M = 0.1, Pr = 0.71, Pm = 0.5, Ha = 2.0, ε = 0.1, λ = - 0.1

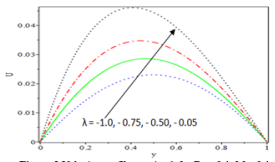

Figure 3 Velocity profile varying λ for Ec = 0.1, M = 0.1, Pr = 0.71, Pm = 0.5, Ha = 2.0, ε = 0.1, V = 0.1

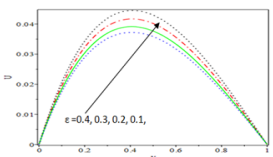

Figure 4 Velocity profile varying ε for Ec = 0.1, M = 0.1, Pr = 0.71, Pm = 0.5, Ha = 2.0, λ = - 0.1, V = 0.1

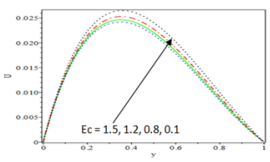

Figure 5 Velocity profile varying Ec for λ = - 0.1, M = 0.1, Pr = 0.7, Pm = 0.5, Ha = 2.0, ε = 0.1, V = 0.1

Figure 2 shows that the velocity increases as the suction parameter decreases. When the suction decreases, the shear within the boundary layer increases. This makes the momentum boundary layer thinner. Hence, the velocity increases. This shows that suction exerts a

retarding influence on the fluid velocity while injection has an accelerating influence on it. Figure 3 illustrates the viscosity variation parameter λ increasing causing the velocity to increase. As mentioned above, increase in the values of λ (which is negative) signifies that viscosity reduces, which makes the velocity to increase. Also, an increase in viscosity parameter causes a decrease in dimensionless viscosity and hence a decrease in viscous forces (which retards fluid motion). This results to inertia forces dominating viscous forces and therefore the fluid accelerates higher. Increased velocity profile is also observed with decreasing thermal conductivity parameter as seen in figure 4. Decreasing the viscous dissipation variation parameter (Ec) results in an enhanced velocity as depicted in figure 5. This occurs because decrease in the Eckert number means an increase in the motion energy of the fluid.

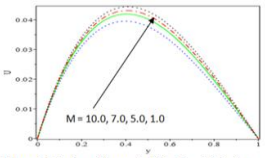

Figure 6 Velocity profile varying M for Ec = 0.5, λ = 0.1, Pr = 0.7, Pm = 0.5, Ha = 2.0, ε = 0.1, V = 0.1

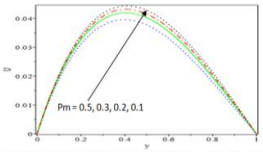

Figure 7 Velocity profile varying Pm for Ec = 0.1, M = 0.1, Pr = 0.7, ε = 0.1, Ha = 2.0, λ = - 0.1, V = 0.1

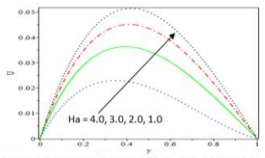

Figure 8 Velocity Profile varying Ha for Ec = 0.1, M = 0.1, Pr = 0.71, Pm = 0.5, λ = -0.1, ε = 0.1, V = 1

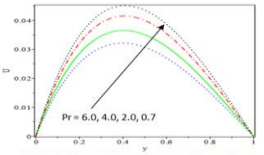

Figure 9 Velocity Profile varying Pr for Ec = 0.1, M = 0.1, Pm = 0.5, Ha = 2.0, ε = 0.1, λ = -0.1

As the magnetic parameter decreases, the flow velocity increases as shown in figure 6. A decrease in transverse magnetic field reduces the development of the opposing force to the flow direction (called the Lorentz force). The result of which is an accelerating force on the velocity field. This also leads to an increased velocity boundary layer thickness. In figure 7, the parameter variation shows that velocity increases as the magnetic prandtl number decreases. When Pm is reduced, the strength of the magnetic induction reduces which makes it possible to achieve increased velocity. Figure 8 depicts decrease in the Hartmann number resulting in increase of the flow velocity. Figure 9 shows that decreasing the prandtl number results in increase in the velocity of the fluid. This occurs because fluids with higher Prandtl number have higher viscosities (and lower thermal conductivities). Implying that, such fluids flow slower than lower Prandtl number fluids. This makes the velocity to decrease significantly with increasing Prandtl number.

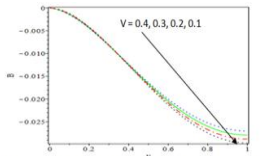

Figure 10 Induced magnetic field profile varying V for Ec = 0.1, M = 0.1, Pr = 0.7, Pm = 0.5, Ha = 2.0, ε = 0.1, λ = - 0.1

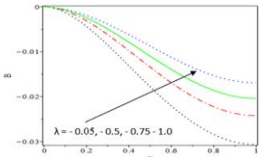

Figure 11 Induced magnetic field profile varying λ for Ec = 0.1, M = 0.1, Pr = 0.7, Pm = 0.5, Ha = 2.0, M = 0.1, ε = 0.1, V = 0.1

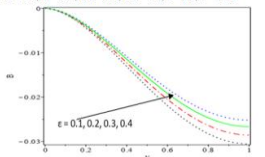

Figure 12 Induced magnetic field profile varying ε for Ec = 0.1, M = 0.1, Pr = 0.71, Pm = 0.5, Ha = 2.0, λ = - 0.1, V = 1.0

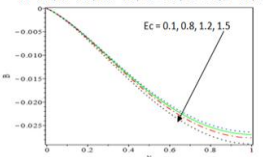

Figure 13 Induced magnetic field profile varying Ec for ε = 0.1, M = 0.1, Pr = 0.71, Pm = 0.5, Ha = 2.0, λ = - 0.1, V = 1.0

In figure 10 it is observed that as the suction parameter decreases, the magnetic induction also decreases. This is a consequence of the reduction of the velocity of flow of the fluid caused by the momentum boundary thickness as the suction decreases. Figure 11, shows that as the viscosity variation parameter decreases; (implying increasing viscosity) the magnetic induction increases. The variation of the thermal conductivity parameter ε as depicted in figure 12 shows that as ε increases, the profile of B increases. Figure 13 displays that as the dissipation parameter (Ec) increases B increases.

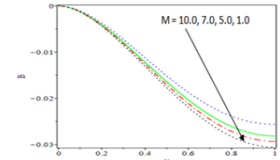

Figure 14 Induced magnetic field profile varying M for Ec = 0.5, ε = 0.1, Pr = 0.71, Pm = 0.5, Ha = 2.0, λ = - 0.1, V = 1.0

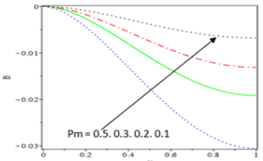

Figure 15 Induced magnetic field profile varying Pm for Ec = 0.1, M = 0.1, Pr = 0.71, ε = 0.1, Ha = 2.0, λ = - 0.1, V = 1.0

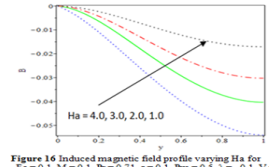

Figure 16 Induced magnetic field profile varying Ha for Ec = 0.1, M = 0.1, Pr = 0.71, ε = 0.1, Pm = 0.5, λ = - 0.1, V = 1.0

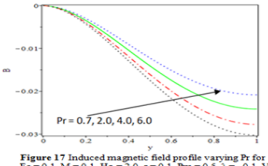

Figure 17 Induced magnetic field profile varying Pr for Ec = 0.1, M = 0.1, Ha = 2.0, ε = 0.1, Pm = 0.5, λ = - 0.1, V = 1.0

The induced magnetic field vary in the same direction as the magnetic parameter as illustrated in figure 14. Decrease in magnetic prandtl number and Hartmann number causes increase in the induced magnetic field shown in figures 15 and 16. Figure 17 shows that as Prandtl number increases, the induced magnetic field also increases.

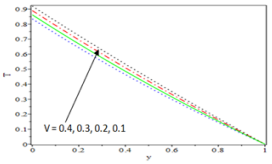

Figure 18 Temperature profile varying V for Ec = 0.1, M = 0.1, Pr =0.71, Pm = 0.5, Ha = 2.0, ε = 0.1, λ = - 0.1

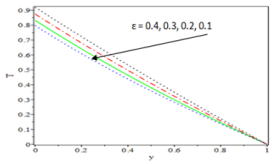

Figure 19 Temperature profile varying ε for Ec = 0.1, M = 0.1, Pr =0.71, Pm = 0.5, Ha = 2.0, V = 1.0, λ = - 0.1

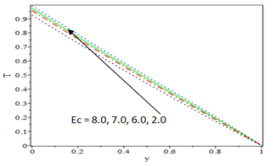

Figure 20 Temperature profile varying Ec for Pr = 0.7, M = 0.1, ε =0.1, Pm = 0.5, Ha = 2.0, V = 1.0, λ = - 0.1

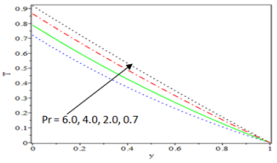

Figure 21 Temperature profile varying Pr for Ec = 0.1, M = 0.1, ε =0.1, Pm = 0.5, Ha = 2.0, V = 1.0, λ = - 0.

The temprature profile depicted in figure 18 shows that it increases as the suction parameter decreases. Decreasing suction causes the increase in thickness of the thermal boundary layer. Therefore, the temperature rises. Figure 19 shows that as the thermal conductivity parameter increases the temprature of the fluid decreases. It is displayed in Figure 20 that the fluid temperature increases as the Eckert number increases. Increase in the kinetic energy increases the molecular interaction in the fluid, which leads to the enhancement of the temperature. Similarly in figure 21, as Pr decreases, the temperature increases. This results because the thermal boundary layer thickness increases with Pr.

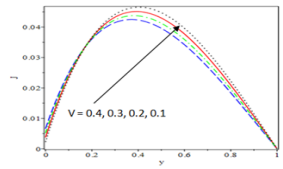

Figure 22 Induced current profile varying V for Ec = 0.1, M = 0.1, Pr = 0.7, Pm = 0.5, Ha = 2.0, ε = 0.1, λ = - 0.1

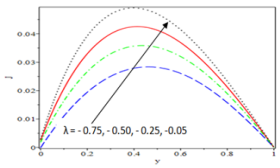

Figure 23 Induced current profile varying λ for Ec = 0.1, M = 0.1, Pr = 0.71, Pm = 0.5, Ha = 2.0, ε = 0.1, V = 1.0

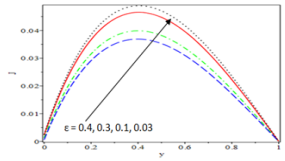

Figure 24 Induced current density varying ε for Ec = 0.1, M = 0.1, Pr = 0.7, Pm = 0.5, Ha = 2.0, λ = - 0.1, V = 0.1

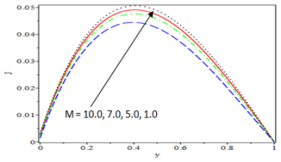

Figure 25 Induced current density varying M for Ec = 0.1, ε = 0.1, Pr = 0.7, Pm = 0.5, Ha = 2.0, λ = - 0.1, V = 0.1

It is observed in figure 22 that as the suction parameter reduces the induced current increases. This result can be explained by the observation above depicted in figure 2 where velocity increases due to reduction in suction. Hence, as the fluid moves faster it generates greater induced current because of the existence of transverse magnetic field in the flow. Figure 23 shows that as the viscosity variation parameter increases, the induced current also increases. An increase in viscosity parameter causes a decrease in dimensionless viscosity and hence reducing viscous forces thereby accelerating the fluid velocity. A faster moving fluid, which conducts electricity passing through a magnetic field, causes increase in the induced current. In figure 24, it is seen that as the thermal conductivity parameter decreases, the induced current increases. Figure 25 shows that, as the magnetic parameter M is reduced J increases. A decreasing magnetic parameter accelerates the velocity of the flow due to the reduction in the magnetic pull caused by the Lorentz force, which develops in the flow field. A consequence of the accelerated velocity of a fluid, which conducts electricity within transverse magnetic field, is the increased generation of induced current density.

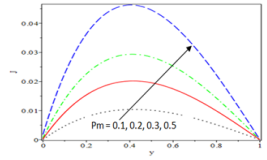

Figure 26 Induced current density varying Pm for Ec = 0.1, M = 0.1 ε = 0.1, Pr = 0.7, Ha = 2.0, λ = - 0.1, V = 0.1

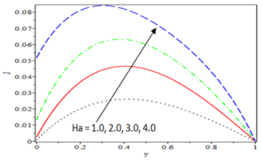

Figure 27 Induced current density varying Ha for Ec = 0.1, M = 0.1, Pr = 0.7, Pm = 0.5, λ = - 0.1, ε = 0.1, V = 1.0

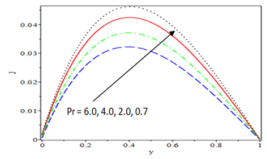

Figure 28 Induced current profile varying Pr for Ec = 0.1, M = 0.1, Pm = 0.5, Ha = 2.0, ε = 0.1, λ = - 0.1, V = 1.0

From the graphs in Figure 26, 27 and 28, it is seen that as Pm and the Hartmann number are increased, the induced current increases. In addition, as the Prandtl number is decreased, the induced current increases too.

Table 2 to 5 above illustrates the consequences of changing the physical parameters namely suction parameter, the Eckert number, magnetic parameter, prandtl number, viscosity variation parameter, thermal conductivity variation parameter, Hartmann and the magnetic prandtl numbers on the coefficient of skin-friction τ, which represent the shearing stress at the plates. Table 6 to 9 represents the values of the heat transfer coefficient Nu obtained after varying the different paramount physical parameters. Table 10 shows a comparison of the present work with [19] where viscosity and thermal conductivity are taken to be constant and viscous dissipation and Ohmic heating are absent.

Table 2 The effect of suction parameter and Prandtl number on the skin friction

λ = -0.1, ε = 0.1, Pr = 0.7 , Pm = 0.5 , Ha = 2.0, Ec = 0.1, M = 0.1			λ = -0.1, ε = 0.1, Pm = 0.5, Ha = 2.0, V = 0.1, Ec = 0.1, M = 0.1		
V	τ_0	τ_1	Pr	τ_0	τ_1
0.1	0.2715610378	0.1104958011	0.7	0.2718017152	0.1130683834
0.2	0.2619721541	0.1013733553	2.0	0.2518087489	0.1027706582
0.3	0.2525234994	0.0927858643	4.0	0.2240854913	0.0889448867
0.4	0.2431903811	0.0846892013	6.0	0.1996612595	0.0773171728

Table 3 The effect of Eckert number and Magnetic parameters on Skin friction

M = 0.1, Pm = 0.5, Ha = 2.0, λ = -0.1, ε = 0.1, Pr = 0.7, V = 1.0			Ec = 0.1, Pm = 0.5, Ha = 2.0, λ = - 0.1, ε = 0.1, Pr = 0.7, V = 1.0		
Ec	τ_0	τ_1	M	τ_0	τ_1
0.1	0.2690839120	0.1105279416	0.1	0.2690839120	0.1105279414
0.8	0.2686334093	0.1087531978	5.0	0.2678570248	0.1092422739
1.5	0.2684952949	0.1072876128	8.0	0.2659576603	0.1072680554
2.8	0.2690885615	0.1053670463	10.0	0.2642208684	0.1054798310

Table 4 The effect of viscosity and thermal conductivity parameters on Skin friction

Ec = 0.1, M = 0.1, Pm = 0.5, Ha = 2.0, ε = 0.1, Pr = 0.7, V = 0.1,			Ec = 0.1, M = 0.1, Pm = 0.5, Ha = 2.0, λ = - 0.1, Pr = 0.7, V = 0.1,		
λ	τ_0	τ_1	ε	τ_0	τ_1
- 0.05	0.2692221381	0.1160585982	0.03	0.2837592488	0.1163618920
- 0.50	0.2569302038	0.1018269319	0.1	0.2715610378	0.1104958011
- 0.75	0.2225755111	0.0933004298	0.30	0.2386828088	0.0955273627
- 1.0	0.1715905946	0.0857110031	0.40	0.2246960041	0.0903161013

Table 5 The effect of Hartmann number and the Magnetic Prandtl number on Skin friction

Ec = 0.1, M = 0.1, Pr = 0.7, ε = 0.1, Pm = 0.5, λ = - 0.1, V = 0.1			Ec = 0.1, M = 0.1, Pr = 0.7, ε = 0.1, Ha = 2.0, λ = -0.1, V = 0.1		
Ha	τ_0	τ_1	*Pm*	τ_0	τ_1
1.0	0.2983531031	0.1322811136	0.05	0.2983910714	0.1338139858
2.0	0.2715610378	0.1104958012	0.10	0.2912794072	0.1281859355
3.0	0.2312728131	0.0757176524	0.20	0.2845230162	0.1229123492
4.0	0.1655568148	0.0110767458	0.35	0.2718017152	0.1130683833

It is observed in table 2 that as suction parameter (V) and the prandtl (Pr) number increases, (τ) decreases on both plates. Increase in suction results in decrease in the shear around the boundary layer. This makes momentum boundary layer thicker. This decreases the flow velocity, causing decrease of the skin friction. In a similar result, τ decreases on both plates when Eckert number (Ec) and the magnetic parameter (M) increases as shown in table 3. In table 4, the effects of the viscosity parameter (λ) and the thermal conductivity parameter (ε) on the (τ) around the two plates is depicted. Decreasing (λ), which means increasing the viscosity of the fluid, results in decrease of the skin friction on both plates. When the viscosity increases, there is a corresponding decrease in the velocity, which causes a decrease in the skin friction. As ε increases, the thermal conductivity decreases, which implies a reduction in the fluid velocity as observed above. Hence, the result is a reduction in the skin friction as is shown in the table. Table 5 shows the effects of Hartmann number (Ha) and (Pm) number on the skin friction. By increasing the (Ha), we observe decrease of the skin friction on both plates. Likewise, increase in Pm number, results in decrease in the skin friction on both plates. This is the case because increasing Ha and Pm slows down the flow velocity.

Table 6 The effects of Eckert number and the magnetic parameter on heat transfer coefficient (Nu)

λ = -0.1, ε = 0.1, Pr = 0.7, Pm = 0.5, Ha = 2.0, M = 0.1, V = 0.1		λ = - 0.1, ε = 0.1, Pr = 0.71 , Pm = 0.5 , Ha = 2.0, Ec = 1.0, V = 0.1	
Ec	Nu	M	Nu
0.1	0.8437553725	0.1	0.8306370290
0.8	0.8247587258	2.8	0.7535531597
1.5	0.8110805330	4.2	0.6589511855
2.8	0.7999620051	6.3	0.4536635710

Table 7 The effect of viscosity and thermal conductivity parameters on heat transfer coefficient (Nu)

Ec = 1.0, M = 0.1, Pm = 0.5, Ha = 2.0, ε = 0.1, Pr = 0.7, V = 0.1		Ec = 1.0, M = 0.1, Pm = 0.5, Ha = 2.0, λ = -0.1, Pr = 0.7, V = 0.1	
λ	Nu	ε	Nu
- 0.005	0.82076767	0.03	0.8929320213
- 0.50	0.87022214	0.1	0.8306370292
- 0.75	0.85825072	0.3	0.6599918028
- 1.0	0.76346717	0.4	0.5946343832

Table 8 The effect of Hartmann and the Magnetic Prandtl numbers on heat transfer coefficient (Nu)

Ec =1.0, M = 0.1, Pr = 0.7, ε = 0.1, Pm = 0.5, λ = - 0.1, V = 0.1		Ec =1.0, M = 0.1 Pr = 0.7, ε = 0.1, Ha = 2.0, λ = - 0.1, V = 0.1	
Ha	Nu	Pm	Nu
1.0	0.8563162222	0.1	0.8474803552
2.0	0.8306370290	0.2	0.8469847886
3.0	0.7600767033	0.3	0.8463703483
4.0	0.6608014643	0.5	0.8447984573

Table 9 The effect of Prandtl number and Suction Parameter on heat transfer coefficient (Nu)

Ec =1.0, M = 0.1, Ha = 2.0, ε = 0.1, Pm = 0.5, λ = - 0.1, V = 0.1		Ec = 1.0, M = 0.1 Pr = 0.7, Pm = 0.5, ε = 0.1, Ha = 2.0, λ = - 0.1	
Pr	Nu	V	Nu
0.7	0.8447984572	0.1	0.8306370289
2.0	0.7411536572	0.2	0.7667898111
4.0	0.6007251699	0.3	0.7051013305
6.0	0.4795460083	0.4	0.6453135136

Table 10 Comparison of the present work with [19]

Sarveshanand and Singh for y = 0.5			Present work for λ = ε = 0 = Ec = M = 0, y = 0.5	
V	U	B	U	B
0.50	0.019475349	0.0248646479	0.0194753493	0.0248646479
0.75	0.016625330	0.0232362671	0.0166253298	0.0232362674
1.00	0.014194754	0.0216757178	0.0141947539	0.02167571800
1.50	0.010355917	0.0187816106	0.0103559175	0.1878161082

To observe the effects of the various parameters on the heat transfer rate, table 6 shows that by increasing the Eckert number, the Nuselt number reduces. While increasing the value of the magnetic parameter Nu increases. Table 7 shows that increasing the thermal conductivity parameter (ε) also results in the increase of the Nusselt number. In table 8, the Hartman number and the magnetic prandtl number effect on the heat transfer rate is depicted. It is seen that as the two parameters increases, the Nusselt number also increases. The same effect is observed when prandtl number and suction parameter are varied as shown on table 9. Table 10 shows the results of the comparison of the present work with [19]. It shows that the results agree to nine places of decimal.

CONCLUSION

The effects of dependent thermal conductivity and viscosity on MHD free convection flow in a vertical porous channel with induced magnetic field is presented in this paper. The effects of various paramount parameters on the velocity field, induced magnetic field, temperature field, induced current density, skin friction profiles and Nusselt number have been depicted in graphs and tables. The findings of this study are as follows:

(1) Reducing the fluid suction and thermal conductivity have similar result as increasing the viscosity of the fluid, the Magnetic Prandtl number and the Hartmann number of retarding the velocity profile of the flow.
(2) Enhancement of the magnetic induction is obtained when the suction is increased, the thermal conductivity is reduced, the prandtl numbers and the Hartmann are increased. It also increases when the viscosity increases and the magnetic prandtl number decreases.
(3) Larger suction results in lower temperature of the fluid. Decreasing temperature profile also results from the increased values of prandtl number.
(4) Lower suction, lower viscosity and lower prandtl number leads to increased induced current density in the fluid. Decreasing profile of the induced current is obtained when the value of the magnetic prandtl number is reduced and the Hartmann number is increased.
(5) Increasing the suction parameter and the prandtl number reduces the skin friction in the two plates.
(6) Increasing the viscosity of the fluid and decreasing the thermal conductivity is to reduce the skin friction in the two plates.
(7) The skin friction on both plates decreases by increasing the Hartmann number and the magnetic Prandtl number.
(8) As the thermal conductivity reduces the rate of heat exchange (convection heat transfer) Nu of the fluid decreases.

REFERENCES

[1] Abdul Quader, Alam M (2015), Effects of Hall Current and Viscous Dissipation on MHD Free Convection Fluid Flow in a Rotating System. AMSE Journals 83(1)110-128
[2] Prasad V. R, A. Subba Rao and Anwar O. B (2014) Computational analysis of viscous dissipation and Joule-heating effects on non-Darcy MHD natural convection flow from a horizontal cylinder in porous media with internal heat generation. Theoret. Appl. Mech. 41(1)37–70
[3] Uwanta I. J. and Hamza M.M. (2014), Effect of Suction and Injection on Unsteady Hydromagnetic Convective Flow of Reactive Viscous Fluid, between Vertical Porous Plates, with Thermal Diffusion. Hindawi Publishing Corporation International Scholarly Research Notices 2014()1-15
[4] Sharma P. R, Manisha Sharma and Yadav R. S. (2014), Viscous Dissipation and Mass Transfer Effects on Unsteady MHD Free Convective Flow along a moving Vertical Porous Plate in the presence of Internal Heat Generation and Variable Suction. International Journal of Scientific and Research Publications, 4(9)2250-3153
[5] Reddy G. V. R; Sekhara K. R and Sitamahalakshmib A. (2015), MHD Free Convection Fluid Flow Past a Semi-Infinite Vertical Porous Plate With Heat Absorption And Chemical Reaction. Int. J. Chem. Sci.: 13(1)525-540
[6] Rogers O. A., Johanna K. S., Jaconiah A. O., James M. O.(2013), MHD Free Convection Flow past a Vertical Infinite Porous Plate in the Presence of Transverse Magnetic Field with Constant Heat Flux. International Journal of Science and Research (IJSR) 2(10)2319-7064
[7] Poonia H And Chaudhary R. C. (2010), MHD Free Convection and Mass Transfer Flow Over an Infinite Vertical Porous Plate with Viscous Dissipation Theoret. Appl. Mech. 37(4)263-287
[8] Singh and Singh (2012) MHD Flow with Viscous Dissipation and Chemical Reaction over a Stretching Porous Plate in Porous Medium International Journal of Engineering Research and Applications (IJERA) 2(2)1556-1564
[9] Das S. S (2009), Effects of Suction and Injection on MHD Three Dimensional Couette Flow and Heat Transfer through a Porous Medium. Journal of Naval Architecture and Marine Engineering 6(2009) 41-51
[10] Subbaiah Naidu K. Ch. V, (2016), Hall Current Effects on Free Convective Flow of Stratified Fluid over an Infinite vertical porous plate, IOSR Journal of Mathematics 12(2016)11-27
[11] Salema A. M and Rania Fathy (2012), Effects of variable properties on MHD heat and mass transfer flow near a stagnation point towards a stretching sheet in a porous medium with thermal radiation, Chinese Physics B 21(5)1-11

[12] Shrama P. R. and Gurminder Singh (2010), Steady MHD Natural Convection Flow with Variable Electrical Conductivity and Heat Generation along an Isothermal Vertical Plate, Tamkang Journal of Science and Engineering 13(3)235-242
[13] Devi S. P. Anjali, B. Ganga (2009) Effects of Viscous and Joules Dissipation on MHD Flow, Heat and Mass Transfer past a Stretching Porous Surface Embedded in a Porous Medium Nonlinear Analysis: Modeling and Control, 14(3)303-314
[14] Hazarika G. C, Santana Hazarika (2015), Effects of variable viscosity and thermal conductivity on magneto hydrodynamics mixed convective flow over a stretching surface with radiation International Journal of Scientific Research Engineering and Technology (IJSRET), 4(7)809-815
[15] Khanday M.A. (2014), Numerical study of partial differential equations to estimate thermoregulation in human dermal regions for temperature dependent thermal conductivity. Journal of the Egyptian Mathematical Society 22(2014)152–155
[16] Sarveshanand and Singh A. K (2015) Magneto hydrodynamic free convection between vertical parallel porous plates in the presence of induced magnetic field Sarveshanand and Singh. Springer Plus 4:333 doi: 10.1186/s40064-015-1097-1
[17] Singh V and Shweta Agarwal (2013)Flow and Heat Transfer of Maxwell Fluid with Variable Viscosity and Thermal Conductivity over an Exponentially Stretching Sheet American Journal of Fluid Dynamics, 3(4)87-95
[18] Gopal Chandra Hazarika, Jadav Konch (2016) Effects of variable viscosity and thermal conductivity on magnetohydrodynamic free convection dusty fluid along a vertical porous plate with heat generation Turkish Journal of Physics 40()52 - 68 doi:10.3906/_z-1509-14
[19] Maple (2016), Maplesoft, a division of Waterloo Maple Inc., Waterloo, Ontario.
[20] Zhou J. K, (1986), Differential transformation and its application for electrical circuits. Huazhong University Press, Wuhan, China.
[21] Hassan I. H. A (2008), Application of differential transformation method for solving systems of differential equations. Applied Mathematical Modeling 32(2008)2552–2559
[22] Batiha A and Batiha B. (2011) Differential Transformation Method for a Reliable Treatment of the Nonlinear Biochemical Reaction Model Advanced Studies in Biology 3(8)355-360
[23] Saeed R. K. and Botan M. Rahman B. M (2011) Differential Transform Method for Solving System of Delay Differential Equation Australian Journal of Basic and Applied Sciences, 5(4)201-206.
[24] Erturk V. S, Zaid M. O, and Momani S (2012) The multi-step differential transform method and its application to determine the solutions of non-linear oscillators. Advances in Applied Mathematics and Mechanics. Adv. Appl. Math. Mech. 4(4)422-438
[25] Oke A. S (2017) Convergence of Differential Transform Method for Ordinary Differential Equations. Journal of Advances in Mathematics and Computer Science. Previously known as British Journal of Mathematics and Computer Science 24(6)1-17.